

# 1 Optically Multiresponsive Heteroleptic Platinum Dithiolene Complex with Proton-Switchable Properties

3 Salahuddin Attar,<sup>†</sup> Davide Espa,<sup>†</sup> Flavia Artizzu,<sup>†</sup> Luca Pilia,<sup>‡</sup> Angela Serpe,<sup>†</sup> Maddalena Pizzotti,<sup>§</sup>  
4 Gabriele Di Carlo,<sup>§</sup> Luciano Marchiò,<sup>||</sup> and Paola Deplano<sup>\*,†,⊥</sup>

5 <sup>†</sup>Dipartimento di Scienze Chimiche e Geologiche and Unità di Ricerca INSTM, Università di Cagliari, S.S. 554-Bivio per Sestu,  
6 I09042 Monserrato-Cagliari, Italy

7 <sup>‡</sup>Dipartimento di Ingegneria Meccanica, Chimica e dei Materiali, Università di Cagliari, Via Marengo 2, I09123 Cagliari, Italy

8 <sup>§</sup>Dipartimento di Chimica and Unità di Ricerca INSTM, Università di Milano, via Golgi 19, I20133 Milano, Italy

9 <sup>||</sup>Dipartimento di Chimica, Università di Parma, Parco Area delle Scienze 17A, I43124 Parma, Italy

10 <sup>⊥</sup>Dipartimento di Fisica and Unità di Ricerca INSTM, Università di Cagliari, S.S. 554-Bivio per Sestu, I09042 Monserrato-Cagliari,  
11 Italy

## 12 **S** Supporting Information

13 **ABSTRACT:** Both linear- and nonlinear-optical properties of  $\text{Bu}_4\text{N}[\text{Pt}(\text{L1})(\text{L2})]$  (**1**;  $\text{L1} = [4',5':5,6][1,4]$ -  
14 dithiino[2,3-*b*]quinoxaline-1',3'-dithiolato;  $\text{L2} = (R)$ - $\alpha$ -  
15 MBActo dithiooxamidate, where  $(R)$ - $\alpha$ -MBA =  $(R)$ -  
16 (+)- $\alpha$ -methylbenzyl) upon HCl addition at room temperature  
17 change dramatically: the color turns from deep blue  
18 to green; the luminescence switches from deep red to  
19 green; the nonlinear-optical response (first hyperpolarizability)  
20 increases by a factor of 12. Thus, **1** behaves as a  
21 unique multiresponsive optical switch whose properties  
22 can be followed by the naked eye.  
23

24 **C**hanges of the linear-optical (LO; absorption and emission  
25 of light)<sup>1</sup> as well nonlinear-optical (NLO)<sup>2</sup> properties in  
26 response to external stimuli are of current scientific interest and  
27 for several applications in devices.<sup>3–5</sup> Molecules suitable for  
28 second-order NLO mostly consist of an electron-donor moiety  
29 connected to an electron-acceptor moiety by a conjugated  $\pi$   
30 bridge.<sup>6</sup> These chromophores show a typical donor–acceptor  
31 (D–A) charge-transfer (CT) transition falling in the low-energy  
32 region. The two moieties may be conveniently functionalized to  
33 enable the on/off switching of a property.<sup>7</sup> Both forms are  
34 required to be stable and easily switchable with a fast response  
35 time. Among the possible molecular switching in D–A-type  
36 chromophores, we have applied our efforts to a molecule where  
37 the acceptor moiety [(*R*)- $\alpha$ -MBActo dithiooxamidate ( $\text{L2}$ ),  
38 where  $(R)$ - $\alpha$ -MBA =  $(R)$ -(+)- $\alpha$ -methylbenzyl] can easily  
39 undergo proton exchange. The donor employed is [4',5':5,6]-  
40 [1,4]dithiino[2,3-*b*]quinoxaline-1',3'-dithiolato ( $\text{L1}$ ). This ligand  
41 may provide the heteroleptic complex with an additional  
42 functionality. In fact, the homoleptic platinum(II) complex  
43 based on this ligand<sup>8</sup> exhibits in solution at room-temperature a  
44 proton-dependent emission at 572 nm well above the energy of  
45 the lowest-energy absorption.<sup>9</sup> The desired product was  
46 prepared as summarized in Scheme S1 in the Supporting  
47 Information (SI), where the characterization of **1** (Figures  
48 S1–S3), as well as X-ray crystallographic measurements and

refinements (Tables S1 and S2 and Figures S4–S6) are  
described.

The molecular structure of **1** comprises the complex anion  
[Pt(L1)(L2)]<sup>−</sup> and the  $\text{Bu}_4\text{N}^+$  cation (Figure 1).  
52 fl

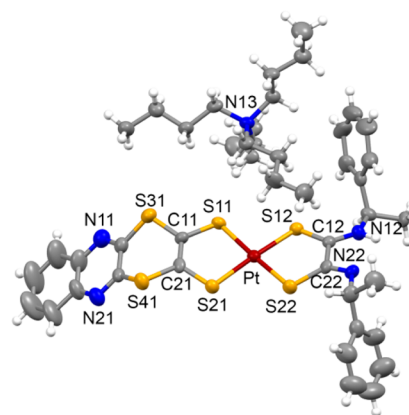


**Figure 1.** Molecular structure of **1** with thermal ellipsoids depicted at the 30% probability level.

The metal exhibits a square-planar geometry, with the Pt–S  
bond distances derived from the quinoxaline ligand slightly  
shorter than those derived from the dithiooxamidate ligand. This  
is in agreement with the different charges of the two ligand  
systems, 2− for the quinoxalinedithiolato system and 1− for the  
dithiooxamidate system. Interestingly, the two SCN moieties of  
the dithiooxamidate system present bond distances that reflect  
monoprotonation of the N(12) atom. Accordingly, the C(22)–  
S(22) fragment exhibits a more pronounced thiolate feature,  
whereas the C(12)–S(12) fragment is characterized by a more  
pronounced thione nature. As far as the LO properties are  
concerned, **1** is characterized by a broad absorption in the visible  
region with medium molar absorption coefficients ( $\epsilon = 5.5 \times 10^3$   
 $\text{M}^{-1} \text{cm}^{-1}$ ) centered at 595 nm in a  $\text{CH}_3\text{CN}$  solution with a 66

**Received:** January 26, 2017

67 shoulder at higher energy ( $\sim 500$  nm) and a quite intense ( $\epsilon =$   
 68  $10.3 \times 10^3 \text{ M}^{-1} \text{ cm}^{-1}$ ) absorption band at 375 nm. Upon the  
 69 addition of HCl, the color of the solution changes from deep blue  
 70 to green. A related substantial change in the absorption profile is  
 71 observed (Figure 2). In particular, the lowest absorption band

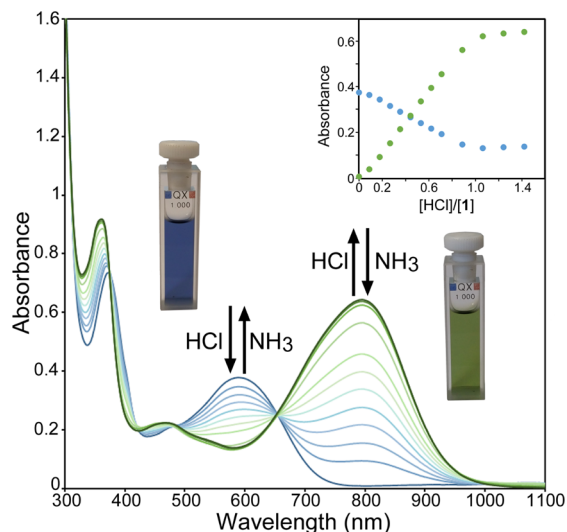


**Figure 2.** Variation of the absorption upon successive additions of HCl ( $10 \mu\text{L}$ ,  $10^{-3} \text{ M}$ ) and  $\text{NH}_3$  ( $10 \mu\text{L}$ ,  $10^{-3} \text{ M}$ ) to a solution of **1** in  $\text{CH}_3\text{CN}$  ( $1 \text{ mL}$ ,  $1 \times 10^{-4} \text{ M}$ ). In the inset, plots of the absorbance values at 588 nm (blue) and 795 nm (green) against  $[\text{HCl}]/[\mathbf{1}]$  are reported.

72 disappears, whereas a new one is formed at higher wavelengths  
 73 (800 nm). The presence of well-defined isosbestic points (at 486  
 74 and 652 nm) suggests that two absorbing species are involved in  
 75 the transformation process, which is complete for a 1:1 molar  
 76 ratio between HCl and **1**. The absorption intensity of the formed  
 77 species (**2**) does not increase upon further HCl addition (see the  
 78 inset in Figure 2).

79 Previous studies by Campagna, Lanza, and co-workers.<sup>10</sup>  
 80 showed that platinum homoleptic complexes coordinated to  
 81  $N,N'$ -dialkyldithiooxamidate ligands formed tight-contact ion  
 82 pairs with  $\text{HX}$  ( $\text{X} = \text{Cl}, \text{Br}, \text{I}$ ), where the  $\text{N}\cdots\text{H}\cdots\text{X}$  interactions play  
 83 a role in stabilizing the ion-pair species. Also in the present case,  
 84 HCl addition to **1** solutions results in protonation of the N atom  
 85 on L2, and the  $\text{N}\cdots\text{H}\cdots\text{Cl}$  interactions significantly affect the  
 86 properties of the formed complex anion, **2** ( $\text{X} = \text{Cl}$ ), as supported  
 87 by DFT calculations (vide infra and Figures S7–S10). The trend  
 88 observed in the spectra of **1** upon the addition of different halo  
 89 acids is reported in Figure S11. Density functional theory (DFT)  
 90 and time-dependent DFT (TD-DFT)<sup>11–17</sup> calculations in  
 91  $\text{CH}_3\text{CN}$  allow one to relate the low-frequency peaks mainly to  
 92 a highest occupied molecular orbital (HOMO)–lowest un-  
 93 occupied molecular orbital (LUMO) transition (Figures 3 and  
 94 S9 and S10). A predominant contribution to the HOMO is  
 95 provided by a mixture of  $\pi$ -dithiolate and metal orbitals, while a  
 96  $\pi^*$ -dithiooxamidate orbital gives a predominant contribution to  
 97 the LUMO (LL'CT = ligand-to-ligand charge transfer with some  
 98 metal contribution). When **1** interacts with HCl, the HOMO  
 99 energy is not affected while the LUMO is stabilized in agreement  
 100 with the observed shift to longer wavelength of the CT band. It is  
 101 worth noting that the LUMO+1, a  $\pi$  orbital of the quinoxaline  
 102 moiety, is raised in energy.

103 Upon irradiation in the visible region at 450 nm, the complex  
 104 shows switchable proton-dependent photoluminescence in

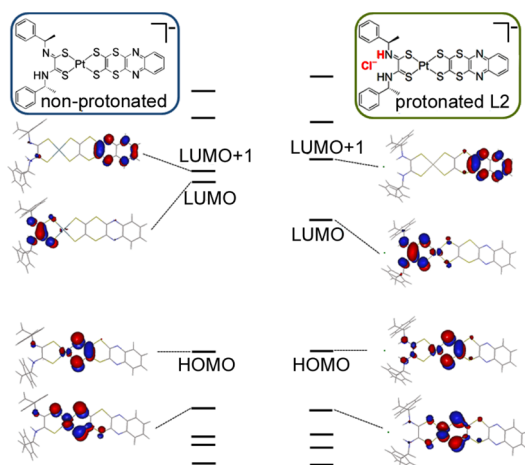


**Figure 3.** Frontier molecular orbitals of **1** (left) and **2** (right). Calculations were performed with the PCM method in acetonitrile, B3LYP/6-31+G(d)-SDD.<sup>11</sup>

solution at room temperature (Figure 4). The emission color  
 can be tuned from deep red (715 nm) to bright green (570 nm)

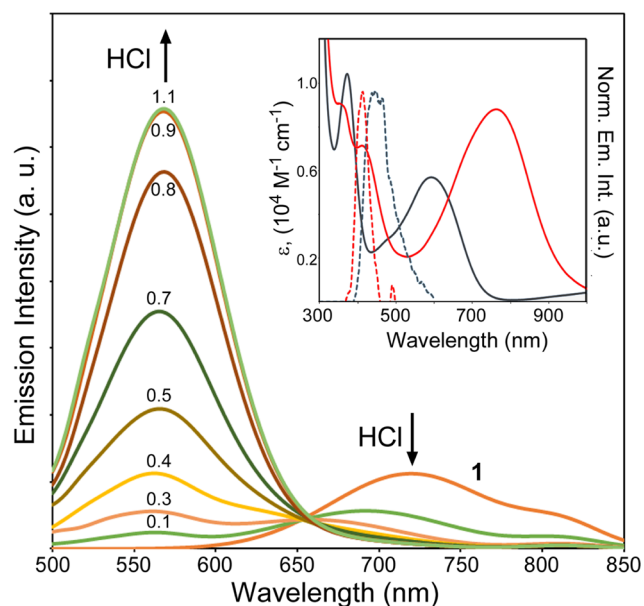


**Figure 4.** Emission change upon successive additions of HCl ( $10 \mu\text{L}$ ,  $10^{-2} \text{ M}$ ) to a solution of **1** in  $\text{CH}_3\text{CN}$  ( $1.5 \text{ mL}$ ,  $5 \times 10^{-4} \text{ M}$ ). Molar ratios  $[\text{HCl}]/[\mathbf{1}]$  are indicated. The excitation wavelength was 450 nm. In the inset, the excitation spectra (dashed lines) are compared to the absorption spectra (solid lines) in a  $\text{CH}_3\text{CN}$  solution of **1** (black) and **2** (red).

upon the addition of 1 equiv of HCl, while the subsequent  
 addition of  $\text{NH}_3$  totally quenches the green band and restores the  
 initial conditions (see Figure S12). Interestingly, both of these  
 emissions are dependent on the excitation wavelength (see the  
 inset in Figure 4), and no photoluminescence is detected upon  
 excitation of the lowest absorption band corresponding to the  
 HOMO–LUMO transition as well as in the UV part of the  
 absorption spectrum. These results may suggest an unusual anti-  
 Kasha–Vavilov behavior<sup>18–20</sup> for **1** in the both unprotonated and  
 protonated forms<sup>21</sup> (see also Figure S13).

A similar behavior was recently found for the homoleptic  
 platinum complex with ligand L1,  $[\text{Pt}(\text{L1})_2]^-$ .<sup>8</sup> In this last case, 118

119 irradiation at 420 nm under neutral conditions in a solution at  
120 room temperature yields an emission peak at 572 nm, which is  
121 well above the energy to the lowest absorption peak at 1085 nm  
122 associated with the HOMO-1  $\rightarrow$  SOMO transition. Emission  
123 was attributed to the HOMO-1  $\leftarrow$  LUMO transition, involving  
124 orbitals localized on the quinoxaline moiety. On the other hand,  
125 the homoleptic [Pt(HL2)<sub>2</sub>] complex is nonluminescent in the  
126 neutral form. This complex becomes emissive at 700 nm upon  
127 HCl addition as a contact ion pair formulated as [Pt(H<sub>2</sub>-R<sub>2</sub>-  
128 dtO)<sub>2</sub>]<sup>2+</sup>(Cl)<sub>2</sub>.<sup>22,23</sup> Reversibility of this property is also observed  
129 upon NH<sub>3</sub> addition. Therefore, a comparison of the emissive  
130 properties of **1** with respect to the corresponding homoleptic  
131 complexes as well as the sequence of molecular orbitals (Figures  
132 **3** and S10) suggests that the process originates mainly from  
133 intraligand charge-transfer (ILCT) transitions involving L1  
134 orbitals of the dithiolate moiety, with some metal contribution,  
135 and the ligand periphery localized on the quinoxaline moiety  
136 (LUMO+1) in both **1** and **2**, similarly to [Pt(L1)<sub>2</sub>]<sup>-</sup>. In the  
137 present case, L2 acts as a reversible proton acceptor, and the  
138 synergistic combination of the two ligands L1 and L2 allows  
139 tuning of the emission color of L1 through the proton-switchable  
140 properties of L2. The rather low quantum yields evaluated  
141 through the relative method ( $6.4 \times 10^{-5}$  for **1** and  $1.4 \times 10^{-4}$  for  
142 **2**) and the room temperature decay times estimated from  
143 spectral data falling in the picosecond range (14 ps for **1** and 4 ps  
144 for **2**; see the SI and Table S3) point out that the radiative decay  
145 channel in both **1** and **2** is strongly quenched by other  
146 deactivation pathways. Therefore, it must be underlined that  
147 the term "anti-Kasha" emission is herein used with caution to  
148 describe an apparent phenomenon related to the observed  
149 spectral features. Transient absorption experiments currently  
150 underway will help to clarify the peculiar photocycle leading to  
151 the apparent anti-Kasha emission in this complex.

152 In addition to these LO properties, **1** exhibits also proton-  
153 switchable NLO properties. Protonation-deprotonation NLO  
154 switches in solution are commonly studied by the hyper-  
155 Rayleigh-scattering (HRS) technique working at 1064 nm  
156 incident wavelength, which, however, suffers the limitation of  
157 possible overestimation of the value of the quadratic hyper-  
158 polarizability due to resonance.<sup>24-26</sup> To achieve more reliable  
159 data, the electric-field-induced second-harmonic-generation  
160 (EFISH) technique was employed to determine the second-  
161 order NLO response of the molecular chromophore **1** in CHCl<sub>3</sub>  
162 solutions, working at a nonresonant 1907 nm incident  
163 wavelength, from which  $\mu\beta_{\lambda}$  can be obtained,<sup>27</sup> (see the SI for  
164 experimental details).<sup>28</sup> More recently, a second-order NLO  
165 response by the EFISH technique has been reported for  
166 protonation-deprotonation NLO switches applied to organic<sup>29</sup>  
167 and organometallic<sup>30</sup> compounds. A remarkable  $\mu\beta_{1907}$  value  
168 increase for **1** by a factor of 4 (from  $-735 \times 10^{-48}$  esu for **1** to  
169  $-2980 \times 10^{-48}$  esu for **2**) is obtained. By taking into  
170 consideration the calculated  $\mu$  value for **1** and **2** (12.6 and 3.9  
171 D, respectively), the obtained  $\beta$  values show an increase by a  
172 factor of 12 ( $60$  and  $735 \times 10^{-30}$  esu for **1** and **2**, respectively). It  
173 is worth noting that the  $\mu\beta_{\lambda}$  value determined on the 1-HCl  
174 solution after NH<sub>3</sub> addition suggests that the NLO-phore **1** is  
175 restored. The negative sign of  $\mu\beta_{\lambda}$  values is in agreement with a  
176 decrease of the dipolar moments in the excited states, as reflected  
177 by the negative solvatochromism observed for the involved CT  
178 peaks (Figure S14). Similar behavior was observed for  
179 M(diimine)(dithiolate) complexes,<sup>31</sup> that have been largely  
180 investigated by Eisenberg's group and others for their NLO<sup>32-34</sup>  
181 and luminescent properties<sup>32</sup> and as sensitizers or photocatalysts

for light-to-chemical energy conversion.<sup>35-37</sup> Several organ-  
ic<sup>24-26,38-41</sup> and organometallic<sup>30,42-47</sup> molecules based on  
D- $\pi$ -A moieties have been shown to undergo a variation of  
hyperpolarizability upon variation of the D-A strength or of the  
 $\pi$  bridge induced by external stimuli, including protonation.  
Similarly, proton-switchable emission has been found.<sup>18,48,49</sup>  
Remarkably, in the case under discussion, color, second-order  
NLO response, and emission all undergo switching upon  
protonation.

In conclusion, **1** behaves as a versatile multiresponsive optical  
switch. Coordination to the metal ion of L1 and L2, each of them  
a carrier of functionality, in a square-planar geometry allows one  
to reach a favorable arrangement for second-order NLO and for  
reversible interactions with HCl through L2. These interactions  
affect both the LO and NLO properties. This peculiarity is  
accompanied by an uncommon behavior of the emission  
properties of **1**. Thus, **1** represents a unique candidate that  
should stimulate interest in deepening its remarkable properties  
both for pure scientific reasons and for potential applications as a  
multiresponsive optical switch whose changes, accompanied by  
color tuning, can be followed by the naked eye.

## ■ ASSOCIATED CONTENT

### 📄 Supporting Information

The Supporting Information is available free of charge on the  
ACS Publications website at DOI: 10.1021/acs.inorg-  
chem.7b00238.

Preparation and characterization of **1**, details on X-ray  
crystallography, DFT and TD-DFT computational  
studies, additional absorption and emission spectra  
including those of L1, photophysical parameter evaluation,  
details on NLO measurements, and solvatochromism  
(PDF)

### Accession Codes

CCDC 1497428 contains the supplementary crystallographic  
data for this paper. These data can be obtained free of charge via  
[www.ccdc.cam.ac.uk/data\\_request/cif](http://www.ccdc.cam.ac.uk/data_request/cif), or by emailing [data\\_](mailto:data_request@ccdc.cam.ac.uk)  
[request@ccdc.cam.ac.uk](mailto:request@ccdc.cam.ac.uk), or by contacting The Cambridge  
Crystallographic Data Centre, 12 Union Road, Cambridge  
CB2 1EZ, UK; fax: +44 1223 336033.

## ■ AUTHOR INFORMATION

### Corresponding Author

\*E-mail: [deplano@unica.it](mailto:deplano@unica.it). Phone: +39 070 675 4680.

### ORCID

Angela Serpe: 0000-0002-3476-0636

Paola Deplano: 0000-0002-8861-8619

### Notes

The authors declare no competing financial interest.

## ■ ACKNOWLEDGMENTS

The authors warmly thank Prof. A. Cannizzo for helpful  
discussion regarding anti-Kasha behavior and Prof. S. Lanza  
regarding ligand L2 features. This research was supported by  
Fondazione Banco di Sardegna. Thanks are also due to COST  
Action CM1202, PERSPECT-H2O.

## ■ REFERENCES

(1) You, J.; Kim, J.; Park, T.; Kim, B.; Kim, E. Highly Fluorescent  
Conjugated Polyelectrolyte Nanostructures: Synthesis, Self-Assembly,  
and Al<sup>3+</sup> Ion Sensing. *Adv. Funct. Mater.* **2012**, *22*, 1417-1424.

- 239 (2) van Bezouw, S.; Campo, J.; Lee, S.-H.; Kwon, O.-P.; Wenseleers,  
240 W. Organic Compounds with Large and High-Contrast pH-Switchable  
241 Nonlinear Optical Response. *J. Phys. Chem. C* **2015**, *119*, 21658–21663.
- 242 (3) Mori, T.; Okamoto, K.; Endo, H.; Hill, J. P.; Shinoda, S.;  
243 Matsukura, M.; Tsukube, H.; Suzuki, Y.; Kanekiyo, Y.; Ariga, K.  
244 Mechanical Tuning of Molecular Recognition To Discriminate the  
245 Single-Methyl-Group Difference between Thymine and Uracil. *J. Am.*  
246 *Chem. Soc.* **2010**, *132*, 12868–12870.
- 247 (4) Campagnola, P. Second harmonic generation imaging microscopy:  
248 Applications to diseases diagnostics. *Anal. Chem.* **2011**, *83*, 3224–3231.
- 249 (5) Best, Q. A.; Sattenapally, N.; Dyer, D. J.; Scott, C. N.; McCarroll,  
250 M. E. pH-Dependent Si-Fluorescein Hypochlorous Acid Fluorescent  
251 Probe: Spirocyclic Ring-Opening and Excess Hypochlorous Acid-  
252 Induced Chlorination. *J. Am. Chem. Soc.* **2013**, *135*, 13365–13370.
- 253 (6) Goovaerts, E.; Wenseleers, W. E.; Garcia, M. H.; Cross, G. H.  
254 Handbook of Advanced Electronic and Photonic Materials and Devices.  
255 In *Nonlinear Optical Materials*; Nalwa, H. S., Ed.; Academic Press: New  
256 York, 2001; Vol. 9.
- 257 (7) Asselberghs, I.; Clays, K.; Persoons, A.; Ward, M. D.; McCleverty, J.  
258 Switching of molecular second-order polarizability in solution. *J. Mater.*  
259 *Chem.* **2004**, *14*, 2831–2839.
- 260 (8) Attar, S.; Espa, D.; Artizzu, F.; Mercuri, M. L.; Serpe, A.; Sessini, E.;  
261 Concas, G.; Congiu, F.; Marchiò, L.; Deplano, P. A Platinum-Dithiolene  
262 Monoanionic Salt Exhibiting Multiproperties, Including Room-  
263 Temperature Proton-Dependent Solution Luminescence. *Inorg. Chem.*  
264 **2016**, *55*, 5118–5126.
- 265 (9) Kasha, M. Characterization of electronic transitions in complex  
266 molecules. *Discuss. Faraday Soc.* **1950**, *9*, 14–19.
- 267 (10) Giannetto, A.; Puntoriero, F.; Barattucci, A.; Lanza, S.; Campagna,  
268 S. Tight-contact ion pairs involving Pt(II) dithioamide complexes:  
269 The acid-base reactions between hydrohalogenated ion-paired com-  
270 plexes and pyridine. *Inorg. Chem.* **2009**, *48*, 10397–10404.
- 271 (11) Becke, A. D. Density-functional exchange-energy approximation  
272 with correct asymptotic behavior. *Phys. Rev. A: At., Mol., Opt. Phys.* **1988**,  
273 *38*, 3098–3100.
- 274 (12) Becke, A. D. Density-functional thermochemistry. III. The role of  
275 exact exchange. *J. Chem. Phys.* **1993**, *98*, 5648–5652.
- 276 (13) Fuentealba, P.; Preuss, H.; Stoll, H.; Von Szentpaly, L. A proper  
277 account of core-polarization with pseudopotentials: single valence-  
278 electron alkali compounds. *Chem. Phys. Lett.* **1982**, *89*, 418–422.
- 279 (14) Cao, X. Y.; Dolg, M. Segmented contraction scheme for small-  
280 core lanthanide pseudopotential basis sets. *J. Mol. Struct.: THEOCHEM*  
281 **2002**, *581*, 139–147.
- 282 (15) Schwerdtfeger, P.; Dolg, M.; Schwarz, W. H. E.; Bowmaker, G. A.;  
283 Boyd, P. D. W. Relativistic effects in gold chemistry. I. Diatomic gold  
284 compounds. *J. Chem. Phys.* **1989**, *91*, 1762–1774.
- 285 (16) Casida, M. E.; Jamorski, C.; Casida, K. C.; Salahub, D. R.  
286 Molecular excitation energies to high-lying bound states from time-  
287 dependent density-functional response theory: Characterization and  
288 correction of the time-dependent local density approximation ionization  
289 threshold. *J. Chem. Phys.* **1998**, *108*, 4439–4449.
- 290 (17) Tomasi, J.; Mennucci, B.; Cammi, R. Quantum mechanical  
291 continuum solvation models. *Chem. Rev.* **2005**, *105*, 2999–3093.
- 292 (18) Park, Y. I.; Postupna, O.; Zhugayevych, A.; Shin, H.; Park, Y.-S.;  
293 Kim, B.; Yen, H.-J.; Cherukuru, P.; Martinez, J. S.; Park, J. W.; Tretiak, S.;  
294 Wang, H.-L. A new pH sensitive fluorescent and white light emissive  
295 material through controlled intermolecular charge transfer. *Chem. Sci.*  
296 **2015**, *6*, 789–797.
- 297 (19) Tseng, H.-W.; Shen, J.-Y.; Kuo, T.-Y.; Tu, T.-S.; Chen, Y.-A.;  
298 Demchenko, A. P.; Chou, P.-T. Excited-state intramolecular proton-  
299 transfer reaction demonstrating anti-Kasha behavior. *Chem. Sci.* **2016**, *7*,  
300 655–665.
- 301 (20) Scuppa, S.; Orian, L.; Donoli, A.; Santi, S.; Meneghetti, M. Anti-  
302 Kasha's rule fluorescence emission in (2-ferrocenyl)indene generated by  
303 a twisted intramolecular charge-transfer (TICT) process. *J. Phys. Chem.*  
304 **2011**, *115*, 8344–8349.
- 305 (21) The emission behavior of the free ligand L1 and its protonated  
306 form as well as the related discussion are reported in Figure S13 to  
address the concerns of impurities due to possible ligand dissociation  
upon the addition of acid.
- (22) Nastasi, F.; Puntoriero, F.; Palmeri, N.; Cavallaro, S.; Campagna,  
S.; Lanza, S. Solid-state luminescence switching of platinum(ii)  
dithioamide complexes in the presence of hydrogen halide and  
amine gases. *Chem. Commun.* **2007**, 4740–4742.
- (23) Rosace, G.; Giuffrida, G.; Saitta, M.; Guglielmo, G.; Campagna, S.;  
Lanza, S. Luminescence Properties of Platinum(II) Dithioamide  
Compounds. *Inorg. Chem.* **1996**, *35*, 6816–6822.
- (24) Mançois, F.; Pozzo, J.-L.; Pan, J.; Adamietz, F.; Rodriguez, V.;  
Ducasse, L.; Castet, F.; Plaquet, A.; Champagne, B. Two-way molecular  
switches with large nonlinear optical contrast. *Chem. - Eur. J.* **2009**, *15*,  
2560–2571.
- (25) Castet, F.; Champagne, B.; Pina, F.; Rodriguez, V. A multistate  
pH-triggered nonlinear optical switch. *ChemPhysChem* **2014**, *15*, 2221–  
2224.
- (26) Asselberghs, I.; Flors, C.; Ferrighi, L.; Botek, E.; Champagne, B.;  
Mizuno, H.; Ando, R.; Miyawaki, A.; Hofkens, J.; Van der Auweraer, M.;  
Clays, K. Second-harmonic generation in GFP-like proteins. *J. Am.*  
*Chem. Soc.* **2008**, *130*, 15713–15719.
- (27)  $\mu$  is the ground-state dipole moment,  $\beta_{\lambda}$  is the projection along the  
dipole moment axis of the vectorial component  $\beta_{\text{VEC}}$  of the tensorial  
quadratic hyperpolarizability, and  $\lambda$  is the fundamental wavelength of the  
incident photons.
- (28) (a) Alain, V.; Blanchard-Desce, M.; Ledoux-Rak, I.; Zyss, J.  
Amphiphilic polyenic push-pull chromophores for nonlinear optical  
applications. *Chem. Commun.* **2000**, 353–354. (b) Valore, A.; Cariati, E.;  
Dragonetti, C.; Righetto, S.; Roberto, D.; Ugo, R.; De Angelis, F.;  
Fantacci, S.; Sgamellotti, S.; Macchioni, A.; Zuccaccia, D. Cyclo-  
metalated Ir<sup>III</sup> Complexes with Substituted 1,10-Phenanthrolines: A  
New Class of Efficient Cationic Organometallic Second-Order NLO  
Chromophores-. *Chem. - Eur. J.* **2010**, *16*, 4814–4825. (c) Tessore, F.;  
Cariati, E.; Cariati, F.; Roberto, D.; Ugo, R.; Mussini, P.; Zuccaccia, C.;  
Macchioni, A. The Role of Ion Pairs in the Second-Order NLO  
Response of 4-X-1-Methylpyridinium Salts. *ChemPhysChem* **2010**, *11*,  
495–507. (d) Colombo, A.; Locatelli, D.; Roberto, D.; Tessore, F.; Ugo,  
R.; Cavazzini, M.; Quici, S.; De Angelis, F.; Fantacci, S.; Ledoux-Rak, I.;  
Tancrez, N.; Zyss, J. New [(D-terpyridine)-Ru-(D or A-terpyridine)][4-  
EtPhCO<sub>2</sub>]<sub>2</sub> complexes (D = electron donor group; A = electron acceptor  
group) as active second-order non linear optical chromophores. *Dalton*  
*Trans.* **2012**, *41*, 6707–6714.
- (29) (a) Nisic, F.; Colombo, A.; Dragonetti, C.; Fontani, M.;  
Marinotto, D.; Righetto, S.; Roberto, D.; Williams, J. A. G. Highly  
efficient acido-triggered reversible luminescent and nonlinear optical  
switch based on 5- $\pi$ -delocalized-donor-1,3-di(2-pyridyl)benzenes. *J.*  
*Mater. Chem. C* **2015**, *3*, 7421–7427. (b) Cariati, E.; Botta, C.; Danelli,  
S. G.; Forni, A.; Giaretta, A.; Giovannella, U.; Lucenti, E.; Marinotto, D.;  
Righetto, S.; Ugo, R. Solid state and solution fine tuning of the linear and  
nonlinear optical properties of (2-pyrene-1-yl-vinyl)pyridine by  
protonation–deprotonation reactions. *Chem. Commun.* **2014**, *50*,  
14225–14228. (c) Cariati, E.; Dragonetti, C.; Lucenti, E.; Nisic, F.;  
Righetto, S.; Roberto, D.; Tordin, E. An acido-triggered reversible  
luminescent and nonlinear optical switch based on a substituted  
styrylpyridine: EFISH measurements as an unusual method to reveal a  
protonation–deprotonation NLO contrast. *Chem. Commun.* **2014**, *50*,  
1608–1610.
- (30) Boixel, J.; Guerschais, V.; Le Bozec, H.; Chantzis, A.; Jacquemin,  
D.; Colombo, A.; Dragonetti, C.; Marinotto, D.; Roberto, D. Sequential  
double second-order nonlinear optical switch by an acido-triggered  
photochromic cyclometallated platinum(II) complex. *Chem. Commun.*  
**2015**, *51*, 7805–7808.
- (31) Cummings, S. D.; Eisenberg, R. Tuning the Excited-State  
Properties of Platinum(II) Diimine Dithiolate Complexes. *J. Am. Chem.*  
*Soc.* **1996**, *118*, 1949–1960.
- (32) Cummings, S. D.; Eisenberg, R. *Progress in Inorganic Chemistry*;  
Wiley: New York, 2004; Vol. 52, Chapter 6.
- (33) Cummings, S. D.; Cheng, L.-T.; Eisenberg, R. Metalloorganic  
Compounds for Nonlinear Optics: Molecular Hyperpolarizabilities of

- 375 M (diimine) (dithiolate) Complexes (M= Pt, Pd, Ni). *Chem. Mater.*  
376 **1997**, *9*, 440–450.
- 377 (34) Mitsopoulou, C. A. Identifying of charge-transfer transitions and  
378 reactive centers in M(diimine) (dithiolate) complexes by DFT  
379 techniques. *Coord. Chem. Rev.* **2010**, *254*, 1448–1456.
- 380 (35) Islam, A.; Sugihara, H.; Hara, K.; Singh, L. P.; Katoh, R.; Yanagida,  
381 M.; Takahashi, Y.; Murata, S.; Arakawa, H. G.; Fujihashi, G. Dye  
382 Sensitization of Nanocrystalline Titanium Dioxide with Square Planar  
383 Platinum(II) Diimine Dithiolate Complexes. *Inorg. Chem.* **2001**, *40*,  
384 5371–5380.
- 385 (36) Geary, E. A. M.; Yellowlees, L. J.; Jack, L. A.; Oswald, I. D. H.;  
386 Parsons, S.; Hirata, N.; Durrant, J. R.; Robertson, N. Synthesis,  
387 Structure, and Properties of [Pt(II) (diimine) (dithiolate)] Dyes with  
388 3,3', 4,4', and 5,5'-Disubstituted Bipyridyl: Applications in Dye-  
389 Sensitized Solar Cells. *Inorg. Chem.* **2005**, *44*, 242–250.
- 390 (37) Zhang, J.; Du, P.; Schneider, J.; Jarosz, J.; Eisenberg, R.  
391 Photogeneration of Hydrogen from Water Using an Integrated System  
392 Based on TiO<sub>2</sub> and Platinum(II) Diimine Dithiolate Sensitizers. *J. Am.*  
393 *Chem. Soc.* **2007**, *129*, 7726–7727.
- 394 (38) Aubert, V.; Guerschais, V.; Ishow, E.; Hoang-Thi, K.; Ledoux, I.;  
395 Nakatani, K.; Le Bozec, H. Efficient photoswitching of the nonlinear  
396 optical properties of dipolar photochromic zinc(II) complexes. *Angew.*  
397 *Chem., Int. Ed.* **2008**, *47*, 577–580.
- 398 (39) Bogdan, E.; Plaquet, A.; Antonov, L.; Rodriguez, V.; Ducasse, L.;  
399 Champagne, B.; Castet, F. Solvent effects on the second-order nonlinear  
400 optical responses in the keto-enol equilibrium of a 2-hydroxy-1-  
401 naphthaldehyde derivative. *J. Phys. Chem. C* **2010**, *114*, 12760–12768.
- 402 (40) Szaloki, G.; Alévêque, O.; Pozzo, J. L.; Hadji, R.; Levillain, E.;  
403 Sanguinet, L. Indolinoxazolidine: A Versatile Switchable Unit. *J. Phys.*  
404 *Chem. B* **2015**, *119*, 307–315.
- 405 (41) Bondu, F.; Hadji, R.; Szalóki, G.; Alévêque, O.; Sanguinet, L.;  
406 Pozzo, J. L.; Cavagnat, D.; Buffeteau, T.; Rodriguez, V. Huge Electro-/  
407 Photo-/Acidoinduced Second-Order Nonlinear Contrasts From Multi-  
408 addressable Indolinoxazolodine. *J. Phys. Chem. B* **2015**, *119*, 6758–  
409 6765.
- 410 (42) Asselberghs, I.; Clays, K.; Persoons, A.; McDonagh, A. M.; Ward,  
411 M. D.; Mc Cleverty, J. A. In situ reversible electrochemical switching of  
412 the molecular first hyperpolarizability. *Chem. Phys. Lett.* **2003**, *368*, 408–  
413 411.
- 414 (43) Boubekur-Lecaque, L.; Coe, B. J.; Harris, J. A.; Helliwell, M.;  
415 Asselberghs, I.; Clays, K.; Foerier, S.; Verbiest, T. Incorporation of  
416 Amphiphilic Ruthenium(II) Ammine Complexes into Langmuir–  
417 Blodgett Thin Films with Switchable Quadratic Nonlinear Optical  
418 Behavior. *Inorg. Chem.* **2011**, *50*, 12886–12899.
- 419 (44) Di Bella, S.; Oliveri, I. P.; Colombo, A.; Dragonetti, C.; Righetto,  
420 S.; Roberto, D. An unprecedented switching of the second-order  
421 nonlinear optical response in aggregate bis(salicylaldiminato)zinc(II)  
422 Schiff-base complexes. *Dalton Trans.* **2012**, *41*, 7013–7016.
- 423 (45) Zhang, Y. R.; Castet, F.; Champagne, B. Theoretical investigation  
424 of the first hyperpolarizability redox-switching in a ruthenium complex.  
425 *Chem. Phys. Lett.* **2013**, *574*, 42–46.
- 426 (46) Wang, W. Y.; Ma, N. N.; Sun, S. L.; Qiu, Y. Q. Impact of redox  
427 stimuli on ferrocene–buckybowl complexes: switchable optoelectronic  
428 and nonlinear optical properties. *Organometallics* **2014**, *33*, 3341–3352.
- 429 (47) Beaujean, P.; Bondu, F.; Plaquet, A.; Garcia-Amorós, J.; Cusido, J.;  
430 Raymo, F. M.; Castet, F.; Rodriguez, V.; Champagne, B. Oxazines: A  
431 New Class of Second-Order Nonlinear Optical Switches. *J. Am. Chem.*  
432 *Soc.* **2016**, *138*, 5052–5062.
- 433 (48) Alam, P.; Kaur, G.; Chakraborty, S.; Roy Choudhury, A. R.;  
434 Laskar, I. R. Aggregation induced phosphorescence” active “rollover”  
435 iridium(III) complex as a multi-stimuli-responsive luminescence  
436 material. *Dalton Trans.* **2015**, *44*, 6581–6592.
- 437 (49) Pilato, R. S.; van Houten, K. A.; *Progress in Inorganic Chemistry*;  
438 Stiefel, E. L., Ed.; Wiley: New York, 2004; Vol. 52, Chapter 7, pp 369–  
439 397.